Supplemental materials

A disease mutation reveals a role for $Na_V1.9$ in acute itch

Juan Salvatierra, Marcelo Diaz-Bustamante, James Meixiong, Elaine Tierney, Xinzhong Dong, Frank Bosmans

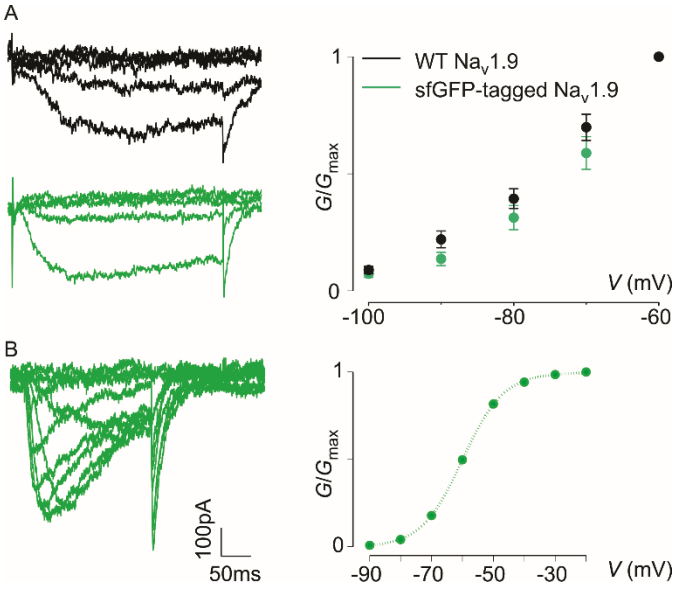

Supplemental Figure 1: Voltage-clamp recordings in DRGs show a similar TTX-R current in WT and sfGFP-$Na_V1.9$ mice. (A) Current traces evoked at hyperpolarized voltages for WT (black) and sfGFP-$Na_V1.9$ (green) show similar kinetics (left) and voltage-dependence of activation (right): $V_{1/2}$ = -61 ± 2mV, slope = 6.5 for WT and $V_{1/2}$ = -65 ± 2mV, slope = 7.6 for sfGFP-$Na_V1.9$ (n=3-5). Due to $Na_V1.8$ current interference, the voltage range is cut off at -60mV (right). Tail currents are visible due to the channel still being open when hyperpolarizing again to -120mV. (B) Representative example of sfGFP-$Na_V1.9$ currents (left) in a DRG with undetectable $Na_V1.8$ current up to -20mV (right). Data in (A) is represented as mean ± SEM.

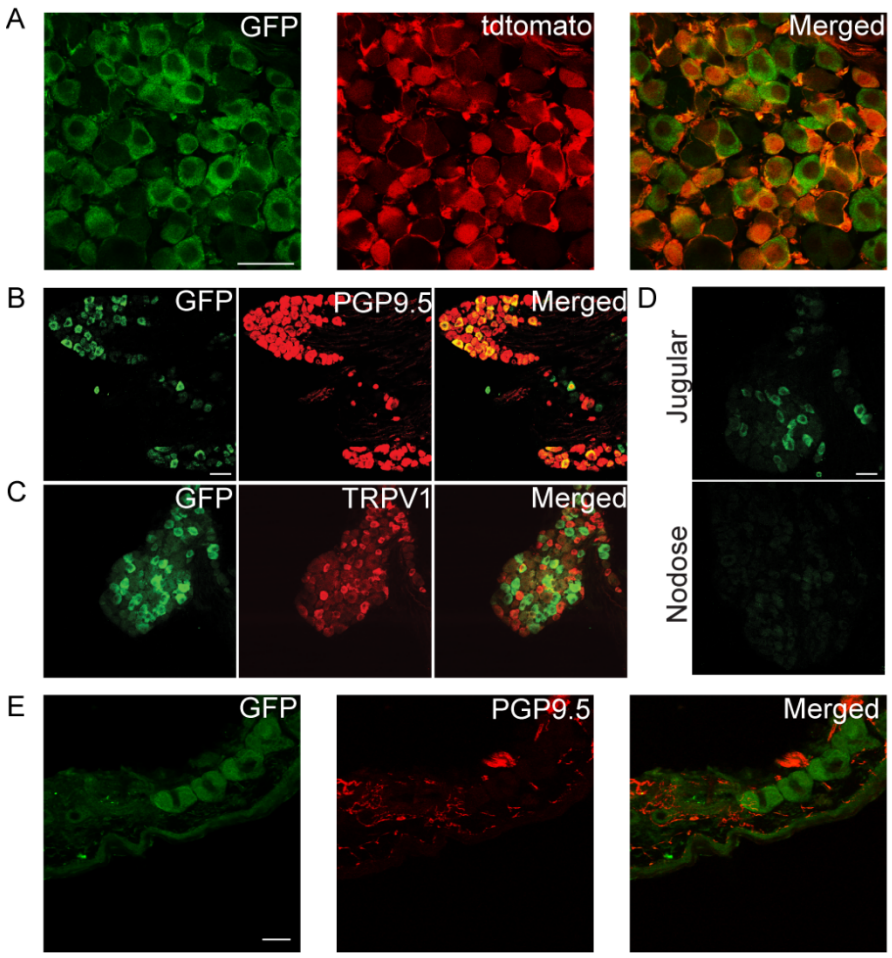

Supplemental Figure 2: $Na_V1.9$ in vagal ganglia and hairy skin. (A) DRG section from a $Na_V1.8Cre^{tdTomato/+}$;sfGFP-$Na_V1.9$ mouse stained against GFP shows large overlap between $Na_V1.8^+$ and $Na_V1.9^+$ neurons. (B-C) $Na_V1.9^+$ neurons overlap with a small subset of $TRPV1^+$ in the jugular ganglia population. (D) $Na_V1.9$ is only seen in the jugular ganglia with no or little expression in the nodose ganglia. (E) Little to no $Na_V1.9$-specific staining is seen in hairy skin of sfGFP-$Na_V1.9$ mice stained against GFP. Scale bars represent 50µm.

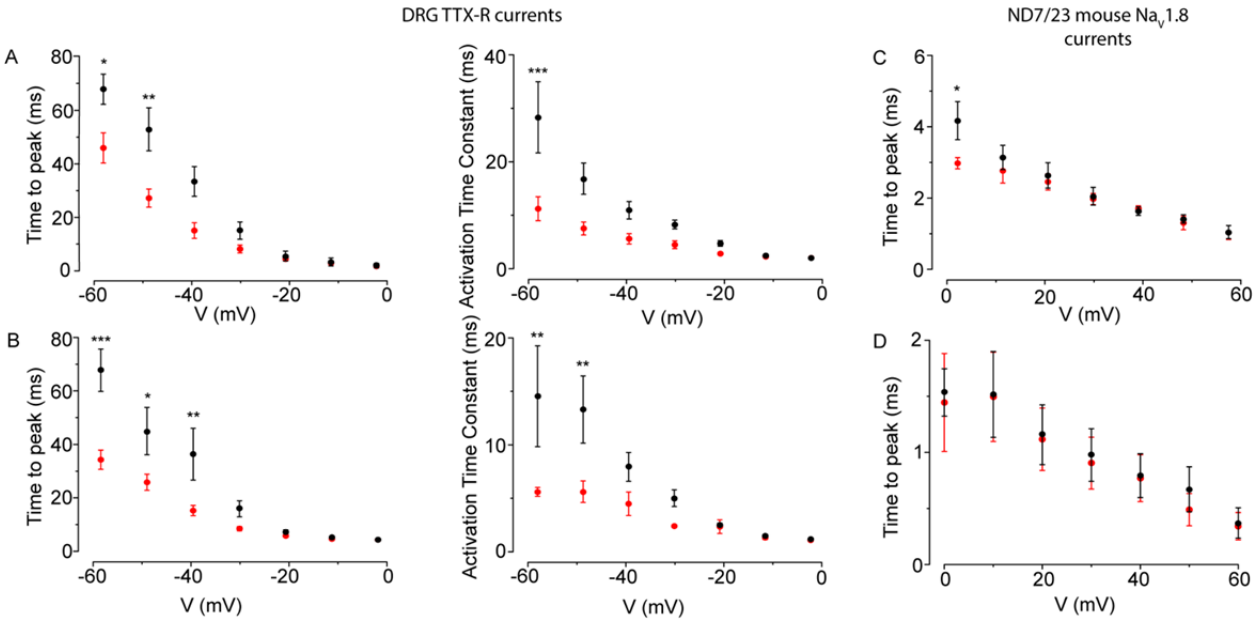

Supplemental Figure 3. Activation of MrgprA3 and MrgprC11 speed up $Na_V1.9$ activation. Electrophysiological recordings from tdTomato$^+$ neurons from MrgprA3$^{tdTomato/+}$ mice. Activation of either MrgprA3 (A) or MrgprC11 (B) with their respective agonist shortened time to peak. Activation time constant is lower for $Na_V1.9$ after MrgprA3 or MrgprC11 activation. These effects are not observed with mouse $Na_V1.8$ co-expressed with either MrgprA3 or MrgprC11, except at 0mV (C, D). Black color is before the addition of compound and red after. Asterisks indicate the results from a two-way ANOVA test followed by Holm-Šídák post hoc analysis. *P<0.05, **P<0.01, and ***P<0.001. Data are represented as mean ± SEM.

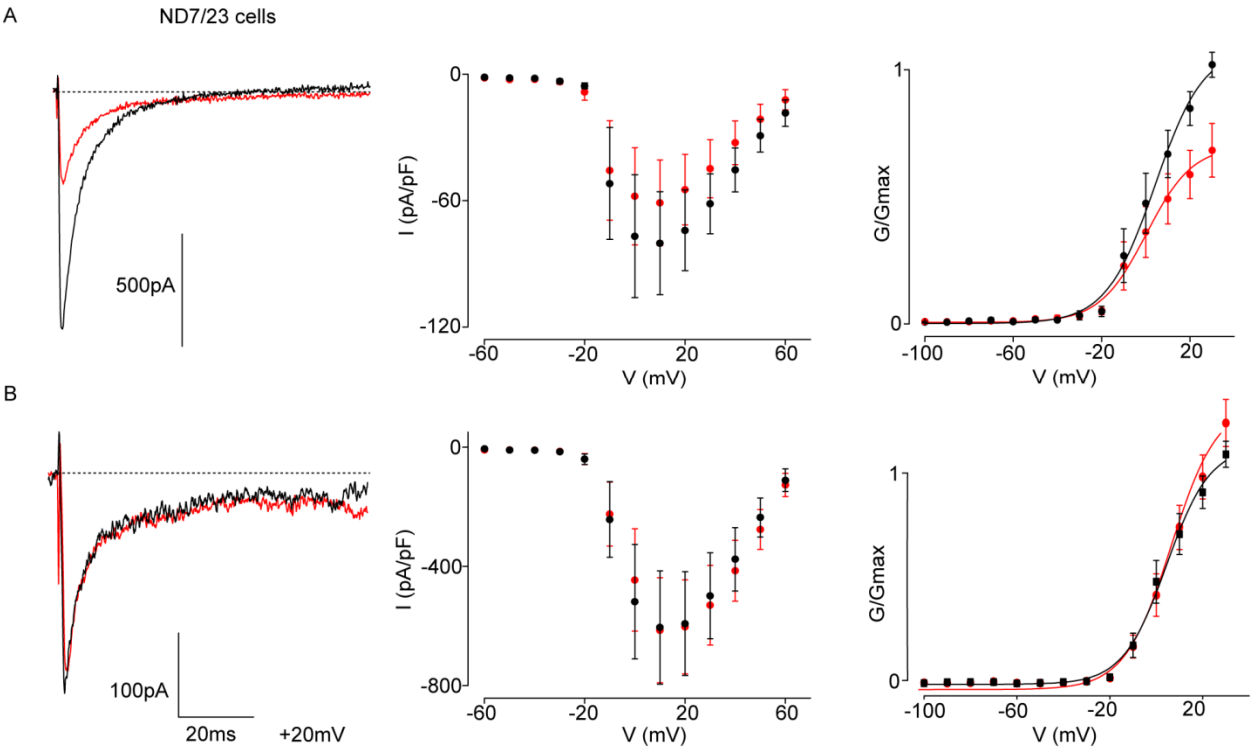

Supplemental Figure 4. MrgprA3 and MrgprC11 activation in ND7/23 cells does not lead to changes in the $Na_V1.8$ activation. Voltage-clamp recordings from ND7/23 cells transfected with mouse $Na_V1.8$ and MrgprA3 or GFP-MrgprC11. (A) Current trace at +20 mV shows effects of CQ on $Na_V1.8$. (A, middle and right panel) Normalized current-voltage (I-V) and (C) conductance-voltage (G-V) relationships before and after CQ application show a similar inhibition of MrgprA3 activation on $Na_V1.8$ as in DRGs, but with no shift in activation voltage (Before $V_{1/2}$ = 7.6 ± 5.3mV; After $V_{1/2}$ = 4.3 ± 5.6mV; n = 8, p = 0.39). (B) Current trace at +20 mV shows no effect of MrgprC11 activation on $Na_V1.8$. (B, middle and right panel) Normalized current-voltage (I-V) and (F) conductance-voltage (G-V) relationships before and after BAM8-22 application show no change in $Na_V1.8$ function in ND7/23 cells (Before $V_{1/2}$ = 6.9 ± 4.2mV; After $V_{1/2}$ = 13.0 ± 4.5mV; n = 8, p = 0.84). Black color is before the addition of compound and red after. Two-tailed paired Student's t-test was used for all. Data are represented as mean ± SEM.

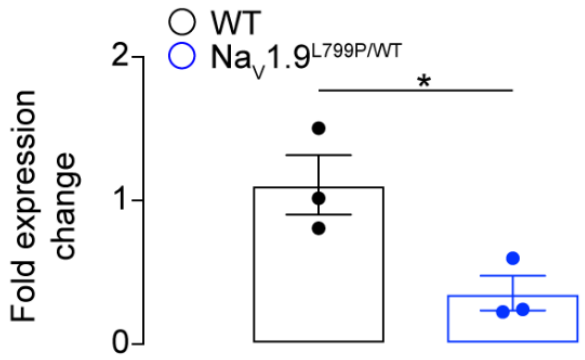

Supplemental Figure 5. qRT-PCR analysis of SCN11A RNA in sfGFP-Na$_V$1.9$^{L799P/WT}$ mice. (A) qRT-PCR analysis on DRGs of sfGFP-Na$_V$1.9$^{L799P/WT}$ mice showed there was about a 68% reduction in SCN11A RNA when compared to littermate controls expressed as change in fold expression compared to WT levels (WT 1.1 ± 0.2, N = 3; sfGFP-Na$_V$1.9$^{L799P/WT}$ 0.36 ± 0.1, N = 3, p = 0.046). *p<0.05, two-tailed unpaired Student's t test. Data are represented as mean ± SEM.